Reduced septal glucose metabolism predicts response to cardiac resynchronization therapy

David Birnie, MB, ChB, MD, Rob A. de Kemp, PhD,
Anthony S. Tang, MD, FRCPC, Terence D. Ruddy, MD, FRCPC, FACC,
Michael H. Gollob, MD, FRCPC, Ann Guo, MEng, Kathryn Williams, MS,
Kerry Thomson, BSc, Jean N. DaSilva, PhD,
and Rob S. Beanlands, MD, FRCPC, FACC

Background. **Up to 50% of patients do not respond to Cardiac Resynchronization Therapy (CRT). Recent work has focused on quantifying mechanical dyssynchrony and left ventricular scar. Septal reverse-mismatch (R-MM) (reduced FDG uptake vs perfusion) has been observed in patients with cardiomyopathy and prolonged QRS duration. We hypothesized that a greater quantity of septal R-MM would indicate a greater potential for reversibility of the cardiomyopathy, when the dyssynchrony is improved with CRT. Therefore, this study's objective was to assess whether greater septal R-MM pattern predicts response to CRT.**

Methods and Results. **Forty-nine patients had pre-implant Rubidium-82 and Fluorine-18-fluorodeoxyglucose PET scanning. Total and regional left ventricular scar size and extent of R-MM were calculated. Response to CRT was defined as ≥10% improvement in left ventricular end-systolic volume or ≥5% absolute ejection fraction improvement. In the non-ischemic cardiomyopathy subset non-responders had significantly less septal R-MM than responders (13.1% compared to 27.1%, $P = .012$). There were correlations between the extent of septal R-MM and the increase in ejection fraction ($r = 0.692$, $P = .0004$) and reduction in left ventricular end-systolic volume ($r = -0.579$, $P = .004$). For each 5% absolute increase in extent of septal R-MM the odds ratio of being a responder was 2.17 (95% CI 1.15, 4.11, $P = .017$). Extent of septal R-MM displayed high sensitivity and specificity (area under curve = 0.855, $P = .017$) to predict response.**

Conclusions. **In patients with non-ischemic cardiomyopathy, greater extent of septal glucose metabolic R-MM pattern, predicted response to CRT. This parameter may be useful for identifying patients who benefit from CRT. (J Nucl Cardiol 2012;19:73–83.)**

Key Words: Bundle-branch block • imaging • metabolism • cardiac resynchronization therapy • response

INTRODUCTION

Cardiac Resynchronization Therapy (CRT) improves quality of life, left ventricular ejection fraction (LV-EF), LV volumes and survival in some patients with advanced congestive heart failure and prolonged QRS.[1-3] However, a number of key questions remain; perhaps most important is the issue of non-response to the therapy. The non-responder rate has been variably estimated to be between 20% and 50%.[4-8] Estimates vary because of differing definitions of response and because of heterogeneity of study cohorts.[4]

Work has focused on quantifying baseline mechanical dyssynchrony (MD) and LV scar. Initial single-center studies suggested that echocardiographic estimation of MD could predict a response to CRT with high sensitivity and specificity.[7,9,10] However, these results have not always been reproducible[5] and newer techniques are being explored with promising initial results.[11,12] Our group and others have observed that the extent of regional or LV scaring also seems important in determining response to CRT.[13-16]

From the University of Ottawa Heart Institute, Ottawa, ON, Canada.
Funding Sources: This study was funded by project Grant from the JP Bickell Foundation and supported in part by a program grant from the Heart and Stroke Foundation of Ontario (HSFO) (#PRG6242). Rob Beanlands is a Career Investigator supported by the HSFO. Dr Tang is a Canadian Institute of Health Research (CIHR) chair.
Received for publication Dec 29, 2010; final revision accepted Nov 5, 2011.
Reprint requests: David Birnie, MB, ChB, MD, University of Ottawa Heart Institute, 40 Ruskin Road, Ottawa, ON K1Y 4W7, Canada; *dbirnie@ottawaheart.ca*.
1071-3581/$34.00

doi:10.1007/s12350-011-9483-8

Left bundle branch block (LBBB) leads to regions of both early and delayed contraction[17-19] which results in reduced work in early activated regions (i.e., the septum) and increased work in late-activated regions (i.e., the LV free wall).[18] Reduced septal work in patients with LBBB is associated with decreased glucose utilization as measured using positron emission tomography (PET) imaging.[20-23] Reduction in septal F-18-fluorodeoxyglucose (FDG) uptake on PET relative to perfusion has been observed in patients with LBBB and cardiomyopathy, so-called reverse-mismatch (R-MM).[23,24] Hence, we hypothesized that a greater quantity of septal R-MM would indicate a greater potential for reversibility of the cardiomyopathy, when the dyssynchrony is improved with CRT. Therefore, this study's objective was to assess whether greater septal R-MM pattern predicts response to CRT.

METHODS

Patients

The study enrolled consecutive consenting patients with LV-EF less than 35% and NYHA Class II or III cardiomyopathy, on optimal medical therapy, with a QRS duration of greater than 130 ms.[16] Ischemic etiology was defined as having both a documented history of myocardial infarction and evidence of significant coronary disease on coronary angiography (at least 1 stenosis $\geq$70% in $\geq$ 2 major arteries). Non-ischemic etiology was defined as no documented history of myocardial infarction and no history suspicious of myocardial infarction and no evidence of significant coronary disease at coronary angiography (no $\geq$ stenosis 50%). Patients who could not be accurately classified were excluded from the study. Patients with right bundle branch block were also excluded.

Study Procedures

The following were obtained prior to CRT implant, 12-Lead ECG; current cardiovascular drug regimen; a Heart Failure assessment using the NYHA Classification; 6-minute hall walk test (6MHW); PET perfusion and metabolism imaging, using Rubidium-82 (Rb-82) for perfusion and F-18-fluorodeoxyglucose (FDG) for metabolism and Equilibrium Radionuclide Ventriculogram (ERVG). All these, with the exception of the PET scan, were repeated 3 months after implant. In addition, patients had echo-guided optimization and device interrogation at 2 weeks and device interrogation at 3-month post-implant. At each time point lead parameters and percentage of bi-ventricular pacing were recorded.

Planar-ERVG—Quantification of LV-EF and LV Volumes

ERVGs were acquired and analyzed using standard techniques blinded to all clinical and other imaging data. The RVGs were acquired with a standard electrocardiogram-gated equilibrium technetium-99m red blood cell blood pool imaging protocol.[25,26] The LV-EF was measured from the left anterior oblique 45° acquisition. LV volumes were determined using the count ratio method.[27]

SPECT-ERVG Imaging and Analysis—Quantification of MD

Data was acquired using standard techniques. In-house software was used to create 568 radial profiles for phase analysis.[28] The program assigns a phase angle to each pixel of the phase image, derived from the first Fourier harmonic of the time-activity curve for that pixel. The phase angle approximates the time at which maximum loss of counts (amplitude) is reached in a pixel,[29] which represents the contraction in that region of the cardiac image.[30] The standard deviation of the phase angles (phaseSD) is a measure of the extent of LV MD.[28]

PET Imaging and Analysis

All patients underwent baseline PET perfusion and metabolism imaging, using Rubidium-82 (Rb-82) for perfusion and F-18-fluorodeoxyglucose (FDG) for metabolism, using established imaging and analysis protocols[25,26,31,32] using an ECAT ART PET (Siemens, Knoxville, TN) or Discovery RX PET/CT (GE Healthcare, Milwaukee, WN). Our standard approach is that patients without diabetes receive oral glucose loading according to the ASNC guidelines[33] and patients with diabetes receive the hyperinsulinemic euglycemic clamp.[34] In the current study, there were 19 patients with Diabetes, 17 of whom received the insulin-euglycemic clamp. One patient with ''borderline'' DM and another with DM did not receive the insulin clamp, but instead oral loading + supplemental Insulin according to the ASNC Guidelines.

All image processing and analysis were performed off-line and the operator was blinded to the patient status. FlowQuant© software was used to reorient images automatically along the long axis of the heart and sample the LV myocardium into polar maps (with 460 sectors) of relative perfusion and FDG uptake (0%-100%).[32] Since our aim was to focus on the septum, the LV polar map was divided into 5 equal area segments; septal, lateral, anterior, posterior, and apex. This ensures that one of the 5 segments included septal myocardium only. An ancillary analysis was also conducted using the standard 17-segment model.

The FDG uptake polar map was normalized by scaling to the average value in the normal perfusion zone; defined as sectors with >75% of the maximum.[25,26,32] The normal zone perfusion and FDG values were then assigned a value of 100%, since this region should not contribute to the perfusion-FDG mismatch scores. The sum of all sector values was used to define the total ''normalized perfusion'' score and the total ''normalized FDG'' uptake score, as developed by our group.[25,26,32] In patients with R-MM (FDG < perfusion) in the septum, the normal zone may include regions with abnormally reduced FDG uptake as shown in Figure 1. This can lead to an incorrect over-normalization of FDG

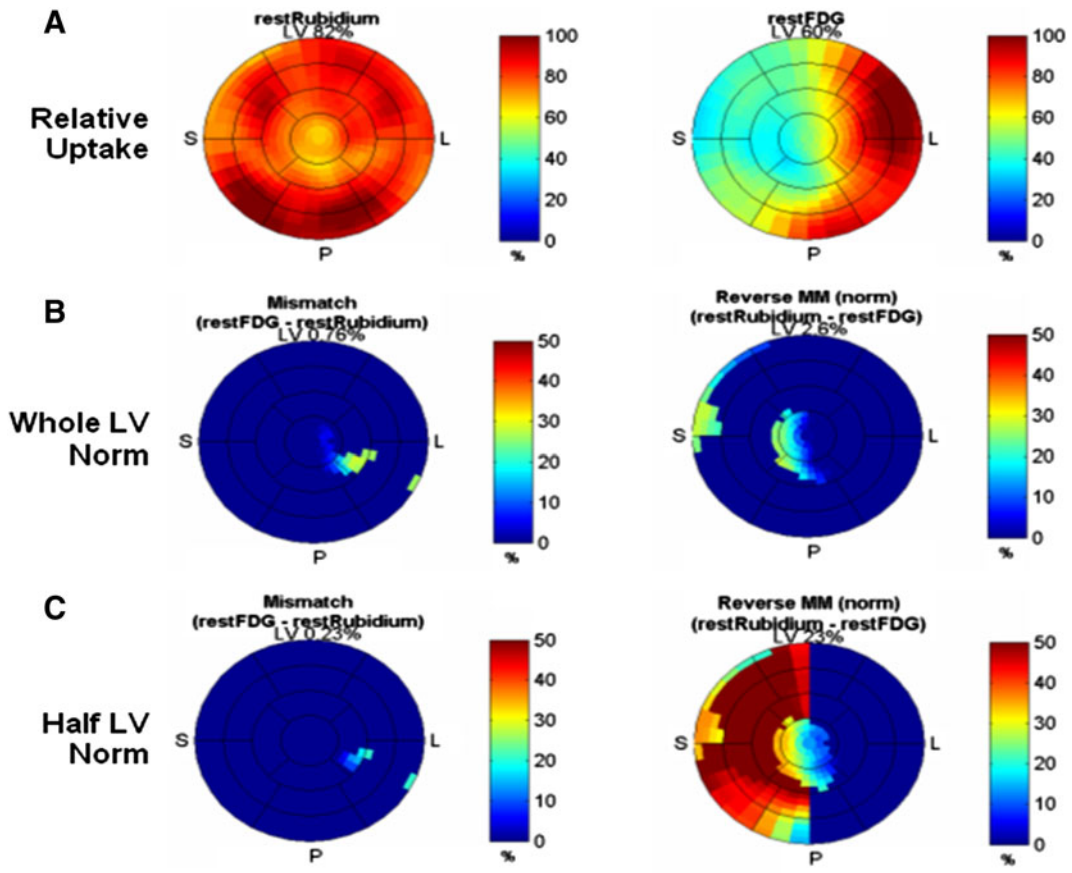

Figure 1. Perfusion-FDG mismatch analyses. Relative perfusion and FDG uptake polar maps demonstrate septal R-MM in a patient with LBBB (**A**). The conventional mismatch analysis severely underestimates R-MM (**B**). The proposed analysis quantifies R-MM in the septum (**C**), with minimal effect on the conventional mismatch (viability) scores. Color scales are 0%-100%. *S*, septum; *L*, lateral wall; *P*, posterior.

uptake, with corresponding over-estimation of mismatch and under-estimation of R-MM. Therefore, we modified the original FDG normalization approach so that the normal perfusion zone could only be selected from the lateral half of the left ventricle.[21] In cases without R-MM, this method does not significantly alter the normalized FDG or traditional mismatch values.

Tissue Characterization

Mismatch and scar. Abnormal perfusion zones were defined as sectors with perfusion <75% of maximum. Within this zone, mismatch (or hibernation) values were defined as the normalized FDG − perfusion difference greater than zero (i.e., FDG > perfusion). Scar values were defined in sectors with abnormal perfusion and incomplete (or partial) mismatch (i.e., 100% − perfusion − mismatch), thereby including sectors with a mixture of scar and hibernating tissues. Scar size was defined as the percentage of sectors with scar values greater than zero.

Reverse-mismatch. R-MM values were calculated for each sector as the perfusion − normalized FDG difference greater than zero (i.e., FDG < perfusion). Global and segmental R-MM scores were determined from the sum of all R-MM sector values, and expressed as a percentage of the LV or segmental total values, respectively.[21] A specific cut point was not used to define an ''abnormal'' cutoff for R-MM. Instead, the continuous values of R-MM were used to enable (i) comparison of the degree of R-MM between responders and non-responders; (ii) determination of relationships of R-MM to other variables; and (iii) ROC analysis to define the degree of R-MM that best predicted a positive response to CRT.

CRT Implantation

The atrial lead was placed in the right atrial appendage, the RV lead was placed at the right ventricular apex. The LV lead was implanted in the lateral or postero-lateral vein.

Echo Optimization of Atrio-Ventricular (AV) and Ventricular-Ventricular (VV) Timing

This was performed using standard methodologies with serial measurements of the aortic flow velocity envelopes.[35]

Definition of Response

This was pre-specified as ≥10% improvement in LVESV (volumes calculated from pre-implant and three months ERVG) or ≥5% absolute improvement in LV-EF. Patients with unsuccessful or unstable lead implantation or dying or being transplanted before their 3-month assessment were excluded from analysis (as pre-specified in the protocol).

Statistical Analysis

Continuous measures are expressed as median and 25th and 75th percentile (Q1, Q3). Categorical measures are presented as frequencies with percentages. The non-parametric Wilcoxon rank sum test for independent samples was performed to identify any significant differences between responders and non-responders to CRT. The correlation of continuous variables was assessed with the Spearman correlation statistic. The Fisher's exact test was used for comparisons between groups.

For the pre-specified secondary stratified analysis of etiology and responder status, subset odds ratios were produced using unadjusted logistic regression with interaction parameters. Receiver operating characteristic (ROC) curves were used to determine cut points for septal that had the optimal sensitivity and specificity to identify response to CRT. A general linear model was used to explore interactions between etiology of cardiomyopathy, responder status, and extent of septal R-MM. A P value <.05 was considered statistically significant. All statistical analyses were performed with SAS version 9.1.3 (SAS Institute Inc., Cary, NC).

Ethics

The protocol received ethics approval from the University of Ottawa Heart Institute ethics board and all patients signed informed consent.

RESULTS

Patients

A total of 51 patients were recruited to the study. One patient died before 3-month follow-up and another had recurrent lead dislodgements. Thus, there were 49 patients for final analysis, 31 responders and 18 non-responders (response rate was 63.3%). In the ICM group, the response rate was 18/27 (66.7%) and in the NICM group 13/22 (59.1%), $P = .58$. Baseline variables stratified by responder status are shown in Table 1. The changes in variables comparing pre-implant to 3-month follow-up are shown in Table 2 (again stratified by responder status).

Quantification of MD

There was no difference in baseline extent of MD between the non-responder and responder groups. There was no change in extent of MD after CRT implantation in the non-responder group (pre-implant 55.8° (42.0, 71.2), post-implant 52.8° (37.6, 67.5), $P = .435$). In the responder group there was a significant reduction in MD from 54.3° (38.4, 67.3) to 31.4° (22.8, 42.9), $P \leq .0001$.

Reduced Glucose Metabolism (R-MM) Quantification—Stratified by Responder Status

The results are shown in Table 3 and Figure 2. Non-responders had significantly less septal R-MM than responders (12.8% (7.9, 22.6) compared to 22.9% (12.2, 33.4) $P = .042$) There was no difference between the groups in extent of other regional R-MM. PET images from one patient are shown in Figure 3.

Reduced Glucose Metabolism (R-MM) Quantification—Stratified by Etiology and Responder Status

In the NICM subset, non-responders had significantly less septal R-MM than responders 13.1%, (8.3, 16.3) compared to 27.1%, (21.8, 33.8), $P = .012$, see Figure 2). There were correlations between the extent of septal R-MM and the increase in LVEF ($r = 0.692$, $P = .0004$, Figure 4A) and reduction in LVESV ($r = -0.579$, $P = .004$, Figure 4B). Also for each 5% absolute increase in extent of septal R-MM the odds ratio of being a responder was 2.17 (95% CI 1.15, 4.11, $P = .017$) (Table 4).

In the ICM group non-responders had less septal R-MM than responders: 12.4%, (7.9, 22.6) compared to 18.2%, (3.9, 27.7), but this was non-significant $P = .54$. There was a modest borderline correlation between extent of septal R-MM and increase of LVEF ($r = 0.371$, $P = .056$). There was no correlation with reduction in LVESV with CRT.

The relationship between etiology of cardiomyopathy, responder status, and extent of septal R-MM was further explored using a general linear model. In the NICM sub-set, there was a significant interaction between responder status and extent of septal R-MM ($P = .012$). In contrast, there was no interaction in the ICM group ($P = .419$).

There were no other differences in the extent of global R-MM or regional R-MM (data not shown), between non-responders and responders in either subset.

Relationship Between Septal Glucose Metabolism (R-MM), Scar, MD, and Other Variables

There were also no differences in RMM score for those who did or did not have the clamp and those who

Table 1. Baseline variables stratified by responder status

	Non-ischemic cardiomyopathy					Ischemic cardiomyopathy				
	Non-responders (n = 9)		Responders (n = 13)			Non-responders (n = 9)		Responders (n = 18)		
Variables	**Median**	**Q1, Q3**	**Median**	**Q1, Q3**	***P* value**	**Median**	**Q1, Q3**	**Median**	**Q1, Q3**	***P* value**
Age	69.0	60.0, 72.0	63.0	58.0, 69.0	.296	69.0	64.0, 78.0	75.0	72.0, 77.0	.570
LV-EF (%)	24.0	11.0, 32.0	23.0	17.0, 30.0	.869	25.0	23.0, 29.0	20.5	14.0, 25.0	.075
LVESV (mL)	236.0	165.0, 302.0	231.0	184.0, 275.0	.817	168.0	149.0, 223.0	219.0	177.0, 256.0	.106
LVEDV (mL)	314.0	242.0, 337.0	328.0	226.0, 332.0	1.000	231.0	197.0, 305.0	267.5	230.0, 324.0	.279
QRS (ms)	166.0	154.0, 190.0	166.0	152.0, 188.0	.766	148.0	128.0, 166.0	174.0	156.0, 182.0	.092
6MHW (m)	281.0	162.0, 335.0	351.0	271.0, 435.5	.110	396.0	312.0, 493.0	300.0	198.0, 333.0	.097
RV pace to LV sense (ms)	145	130, 172	134	125, 148	.252	127	125, 135	145	130, 150	.613
LV pace to RV sense (ms)	140	130, 170	137	125, 175	1.000	140	140, 166	152	142, 190	.225
Mechanical dyssynchrony (°)	55.8	41.5, 71.2	47.7	39.8, 54.6	.300	55.7	42.3, 64.0	67.3	48.9, 73.4	.526
BiV pacing %	99.4	97.8, 99.8	99.6	98.9, 99.9	.155	99.6	98.9, 99.7	99.8	99.2, 99.9	1.000
	n	**%**	**n**	**%**		**n**	**%**	**n**	**%**	
Male	8	88.9	7	53.9	.082	9	100.0	16	94.4	.471
Non-ischemic etiology										
NYHA = III	9	100.0	9	69.2	.066	6	66.7	12	66.7	1.000
LBBB	6	66.7	12	92.3	.125	5	55.6	16	88.9	.056
DM	4	44.4	3	23.1	.290	3	33.3	9	50.0	.411
HTN	3	33.3	4	30.8	.899	6	66.7	11	61.1	.778
Permanent AF	0	0.0	1	7.6	.394	0	0.0	2	11.1	.299
Pre-existing RV pacemaker	3	33.3	1	7.6	.125	2	22.2	1	6.5	.194

6MHW, 6-minute hall walk; *Q1*, *Q3*, 25th and 75th percentile; *LV-EF*, left ventricular ejection fraction; *LVESV*, left ventricular end systolic volume; *LVEDV*, left ventricular end diastolic volume; *LBBB*, left bundle branch block; *NYHA*, New York Heart Association; *RV*, right ventricle.

Table 2. Change in variables (3-month post CRT compared to pre-implant), stratified by responder status

	Non-ischemic cardiomyopathy					Ischemic cardiomyopathy				
	Non-responders (n = 9)		Responders (n = 13)			Non-responders (n = 9)		Responders (n = 18)		
Variables	**Median**	**Q1, Q3**	**Median**	**Q1, Q3**	***P* value**	**Median**	**Q1, Q3**	**Median**	**Q1, Q3**	***P* value**
Δ6MHW (m)	54.0	41.0, 127.0	24.5	9.5, 75.5	.284	−13.0	−99.0, 3.0	59.0	21.0, 95.0	.027
ΔLVEF (%)	1.0	−2.0, 2.0	9.0	8.0, 12.0	.002	1.0	−1.0, 2.0	6.5	2.0, 13.0	.025
ΔLVESV (mL)	16.0	9.0, 33.0	−67.0	−106.0, −44.0	.001	1.0	−5.0, 25.0	−60.5	−82.0, −44.0	.004
ΔLVEDV (mL)	21.0	−8.0, 78.0	−61.0	−117.0, −51.0	.001	9.0	−10.0, 28.0	−67.5	−93.0, −33.0	.009
ΔQRS (ms)	10.0	−10.0, 36.0	−16.0	−26.0, −4.0	.075	−4.0	−10.0, 16.0	−17.0	−38.0, 6.0	.027
ΔNYHA	0.0	−1.0, 0.0	−1.0	−1.0, 0.0	.470	−1.0	−1.0, 0.0	−1.0	−1.0, 0.0	.354
ΔMechanical dyssynchrony (°)	−6.3	−6.8, −5.4	−23.3	−33.3, −11.9	.022	2.3	−1.8, 6.0	−20.1	−34.1, −4.8	.014

Q1, *Q3*, 25th and 75th percentile; *6MHW*, 6-minute hall walk; *LV-EF*, left ventricular ejection fraction; *LVESV*, left ventricular end systolic volume; *LVEDV*, left ventricular end diastolic volume; *NYHA*, New York Heart Association; *RV*, right ventricle.

Table 3. Global and segmental R-MM scores, stratified by responder status

	Non-ischemic cardiomyopathy					Ischemic cardiomyopathy				
	Non-responders (n = 9)		Responders (n = 13)			Non-responders (n = 9)		Responders (n = 18)		
Variables	**Median**	**Q1,Q3**	**Median**	**Q1,Q3**	***P* value**	**Median**	**Q1,Q3**	**Median**	**Q1,Q3**	***P* value**
Global R-MM	5.3	4.7, 9.9	11.7	8.9, 13.5	.036	10.3	6.9, 12.6	7.6	3.6, 14.2	.740
Apical R-MM	5.5	3.4, 11.3	9.0	3.9, 13.1	.312	10.0	4.5, 14.3	5.0	1.4, 10.8	.559
Inferior R-MM	9.8	5.1, 10.7	13.3	10.3, 16.0	.044	14.0	9.3, 16.7	13.4	8.2, 18.1	.878
Lateral R-MM	0.9	0.0, 3.6	0.0	0.0, 0.1		0.6	0.1, 4.4	0.1	0.0, 0.5	
Septal R-MM	13.1	8.3, 16.3	27.1	21.8, 33.8	.012	12.4	7.9, 22.6	18.2	3.9, 27.7	.542
Anterior R-MM	6.5	2.5, 7.9	10.0	5.5, 11.4	.109	6.4	4.1, 7.3	4.8	0.7, 5.1	.389

Q1, *Q3*, 25th and 75th percentile; *R-MM*, reverse-mismatch.

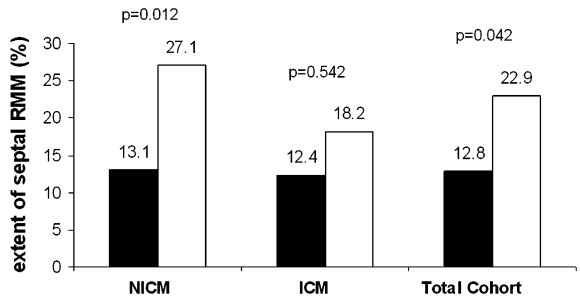

Figure 2. Extent of septal R-MM in sub-sets (*black* non-responders, *white* responders).

did or did not have diabetes. There was a moderate inverse correlation between extent of septal R-MM and extent of septal scar ($r = -0.443$, $P = .0014$). This was consistent in both NICM ($r = -0.410$) and ICM ($r = -0.422$) subsets. ICM patients had significantly more septal scar (40.0%, 7.8, 80.0) than NICM patients (15.5%, 3.4, 36.6, $P = .050$). There were no correlations between the extent of septal R-MM and any of age, etiology, LVEF, QRS duration, extent of MD, or extent of lateral wall scar.

Reduced Septal Glucose Metabolism (R-MM) to Predict Response to CRT

In the NICM subset, a cut point of R-MM extent of 17.2% had 92% sensitivity and 78 % specificity for predicting response to CRT with a negative predictive value of 87.5% and a positive predictive value 85.7%. Figure 5 shows the ROC curve.

Additional Analysis

We repeated the primary analysis (i.e., R-MM Quantification—stratified by etiology and responder status) using the 17-segment standardized ACC/AHA model[36] and found almost identical results (data not shown).

DISCUSSION

In our study, in patients with NICM, the greater reduction of septal glucose metabolism relative to perfusion (septal R-MM) on perfusion-FDG PET imaging, predicted response to CRT. To our knowledge, our study is the first to examine whether septal R-MM

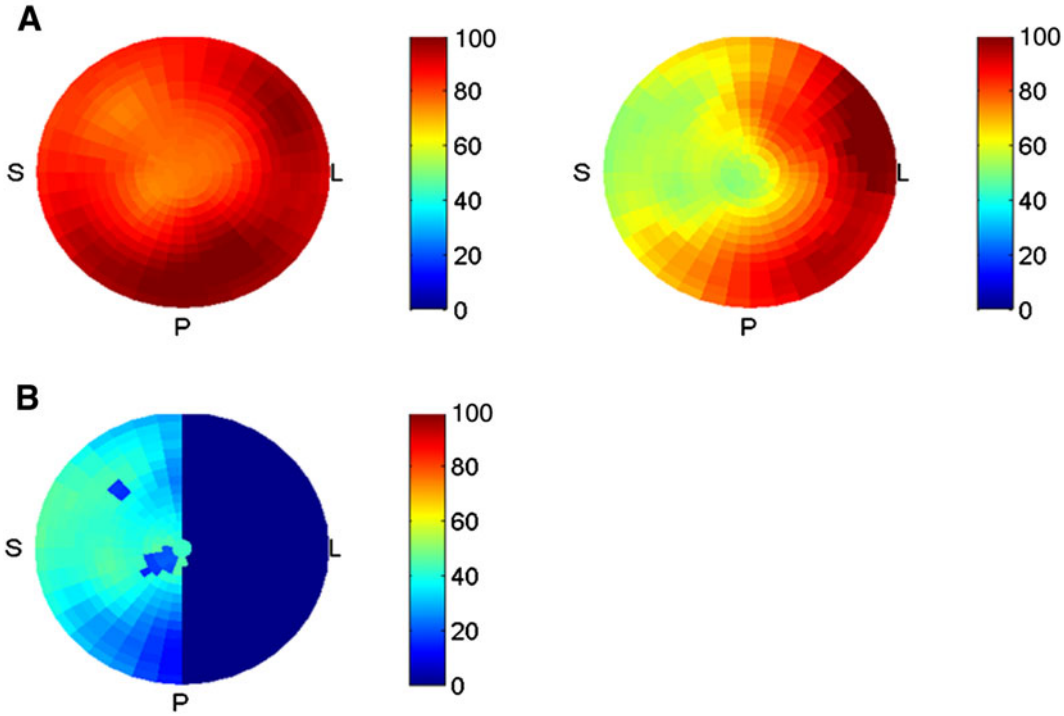

Figure 3. **A**, Example of reconstructed polar maps in a 60-year-old woman with NICM with a pre-implant NYHA Class III, LV-EF of 30%, LVESV 233 mL, and LBBB with QRS duration of 166 ms. The *left panel* shows perfusion and the *right panel* shows FDG uptake. **B**, R-MM map, (a display of the perfusion-FDG) shows is extensive R-MM in the septum with a septal R-MM score of 40.8%. Following CRT, her EF improved to 67% and she improved to NYHA Class I. Color scales are 0%-100%, *S*, septum; *L*, lateral wall; *P*, posterior.

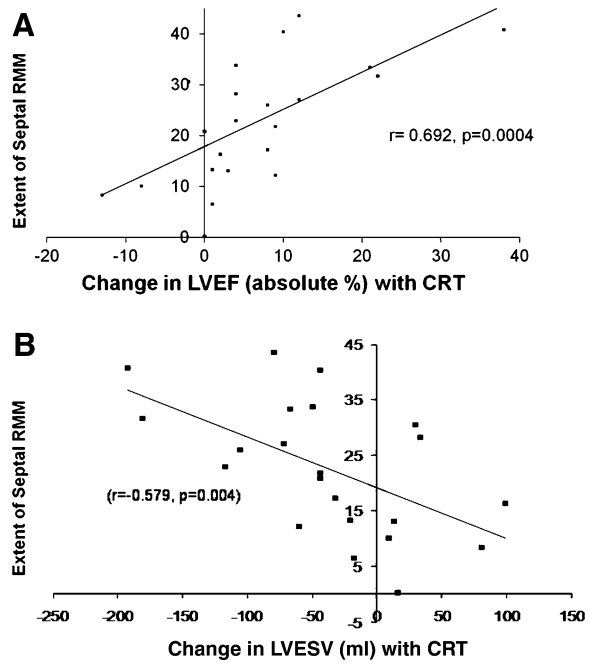

Figure 4. Correlation between extent of septal R-MM and change in LVEF (**A**) and LVESV (mL) (**B**) with CRT in NICM group.

predicts LV remodeling response to CRT. We show that septal R-MM had good sensitivity (92%) and specificity (78%) to predict response to CRT in patients with NICM but not in the ICM group.

Our study supports the preliminary findings of a small pilot study which examined 14 patients (11 NICM, 3 ICM) with spontaneous or pacer-induced LBBB.[20] The survivor group (7 NICM 3 ICM) had significantly more R-MM segments in the septum than the non-survivors (3.3 ± 1.5 vs 0.5 ± 0.6). While this previous pilot study was too small to draw definitive conclusions, it does support our findings regarding the importance of septal R-MM for predicting improvement in the left ventricle.

It is well established that many patients with LBBB and LV dysfunction have reduced septal glucose utilization using FDG PET relative to perfusion imaging.[21,23,24,37,38] This is almost universal in patients with NICM and we have previously shown that it is also common in patients with ICM.[21] While the precise mechanism remains unclear, it appears to be independent of perfusion. Altered transmembrane glucose transport or phosphorylation kinetics have been proposed.[23] As noted by Nowak[23] reductions in septal work would be expected to reduce ATP demand and ergo reduce the need for glucose. Decreased gene expression for GLUT-4 and reduced glucose oxidation have been demonstrated by Depre et al[39] in rats whose hearts have been unloaded by transplantation to the abdominal aorta. This supports that reduction in glucose utilization may be due to unloading effects.[23,39]

There was a moderate inverse correlation between extent of septal R-MM and extent of septal scar. Ischemic cardiomyopathy patients had significantly more septal scar than non-ischemic cardiomyopathy patients. These latter two observations likely explain the non-significant differences in the extent of septal R-MM, between non-responders and responders, in the ischemic cardiomyopathy subgroup

The finding of a moderate inverse correlation between extent of septal R-MM and quantity of septal scar is in contrast to our previous study where we found lateral wall scar was more common in a small group of patients without septal R-MM.[21] These dissimilar observations are likely explained by differences in the study populations. Most importantly the patients in the current study had more extensive scar, both global and regional, than in the previous study. It should also be noted that the relationship between septal scar and septal R-MM can be more readily explained, i.e., with more severe septal scar the amount of perfused myocardium that can have R-MM is reduced. However, we need to study a larger population with a full spectrum of scar extent and R-MM extent to more precisely define the relationship between scar and septal R-MM.

The extent of MD did not predict response to CRT. This may in part reflect our relatively homogeneous

Table 4. Global and segmental scar stratified by responder status

	Non-responders (n = 18)		Responders (n = 31)		
Variables	**Median**	**Q1, Q3**	**Median**	**Q1, Q3**	***P* value**
Global scar size	38.3	29.6, 45.4	35.4	21.5, 49.3	.641
Lateral scar size	24.5	10, 49	5.6	0, 20	.008
Inferior scar size	32.8	18.9, 68.9	24.4	10.1, 47.7	.134
Septal scar size	31.7	7.8, 56.8	34.4	4.4, 56.6	.926
Anterior scar size	26.7	2.2, 47.8	23.4	2.2, 58.8	.585
Apical scar size	62.0	32.0, 73.0	65.0	46.0, 87.0	.227

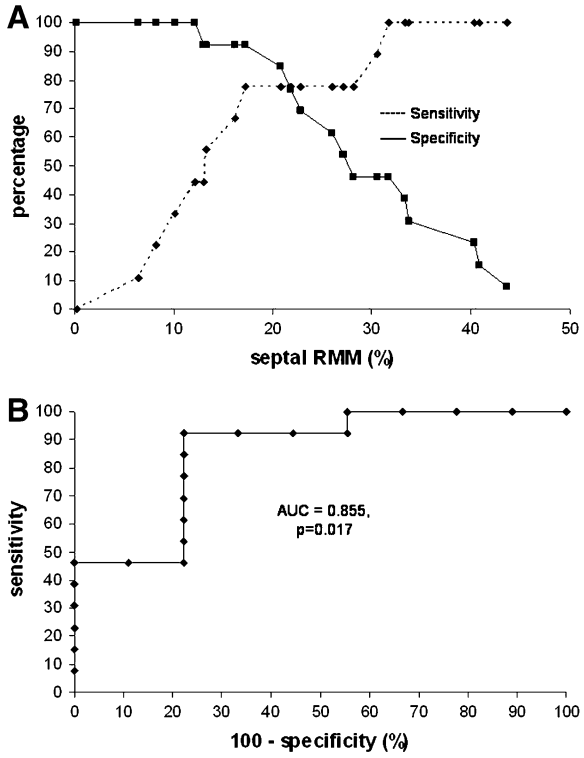

Figure 5. ROC curve analysis in NICM subset on extent of septal R-MM before CRT implantation and response after 3 months of CRT. **A**, Sensitivity curve is *broken line* and specificity is *continuous line*. **B**, There is good predictive value (AUC = 0.855) to predict response.

study population (mostly LBBB, all with QRS greater than 130 ms, no RBBB) and, therefore, likely relatively homogenous extent of MD. We did, however, find the responders had a major reduction in MD and non-responders did not and this is consistent with previous literature.[40] The whole role of MD assessment in predicting response to CRT still needs much clarification and each of the techniques for measuring MD has some advantages and disadvantages. MRI probably provides the most comprehensive measurement of segmental contractions of the ventricles in three dimensions. However, its cost, inaccessibility to many centres, and the inability to perform the test after device implantation are all issues. Newer echocardiographic techniques are being explored with promising initial results.[11,12] Phase imaging of myocardial perfusion studies have the advantage of providing information on both scar and MD.[41,42]

Limitations

The sample size of this study was small but sufficient to address the primary objective which was to determine the association between LV scar, septal R-MM, and response to CRT. This observational study was conducted as a proof of concept pilot for a larger study where the cut point values identified in the current study will be further evaluated. FDG uptake is known to be variable. As such, when perfusion data is acquired with FDG PET, it is often recommended to normalize FDG to regions of maximal perfusion to properly define scar and mismatch. However, the presence of septal R-MM makes approaches for normalization of FDG to perfusion data challenging. There is no standard method for analysis in this scenario. In order to address this, and to facilitate the proof of concept investigation in the current study, we restricted FDG normalization to perfusion values in the lateral half of the ventricle. This or any normalization approach may underestimate R-MM to some degree. Likewise the presence of a very large lateral wall scar could lead to over-normalization. However, it is unlikely that in most circumstances to significantly affect the relationships observed with CRT response. Standardized and normalization approaches to quantify R-MM that also enable accurate measure of match and mismatch, will need to be developed and evaluated in future studies if this concept is to be applied clinically.

Clinical and Research Implications

NICM patients appear to have greater response to CRT than ICM patients.[5,43] We extend this finding by showing that the pathophysiology of LBBB and response to CRT seems to be different in the different populations. In NICM patients, we found that the extent of reverse metabolic mismatch in the septum could have important clinical utility in determining which patients are likely to respond to CRT. These findings require further validation in larger groups of patients before they can be implemented in clinical practice. Also, the relative importance of MD, scar extent, and septal R-MM in different populations needs to be further elucidated.

CONCLUSIONS

In our study, in patients with NICM, the greater reduction of septal glucose metabolism relative to perfusion (septal R-MM) on perfusion-FDG PET imaging, predicted response to CRT. While the mechanism for R-MM remains unclear, this may be a useful parameter in defining patients more likely to respond to CRT.

Acknowledgments

We thank Leslie Carlin for co-ordination of the study; Linda Garrard and May Aung for help with the PET scans and Keri O'Reilly for secretarial assistance.

Conflict of interest

The authors have indicated that they have no financial conflicts of interest.

References

1. Bristow MR, Saxon LA, Boehmer J, Krueger S, Kass DA, De Marco T, et al. Cardiac-resynchronization therapy with or without an implantable defibrillator in advanced chronic heart failure. N Engl J Med 2004;350:2140-50.
2. Cleland JG, Daubert JC, Erdmann E, Freemantle N, Gras D, Kappenberger L, et al. The effect of cardiac resynchronization on morbidity and mortality in heart failure. N Engl J Med 2005;352:1539-49.
3. McAlister FA, Ezekowitz J, Dryden DM, Hooton N, Vandermeer B, Friesen C, et al. Cardiac resynchronization therapy and implantable cardiac defibrillators in left ventricular systolic dysfunction. Evid Rep Technol Assess (Full Rep) 2007;152:1-199.
4. Birnie DH, Tang AS. The problem of non-response to cardiac resynchronization therapy. Curr Opin Cardiol 2006;21:20-6.
5. Chung ES, Leon AR, Tavazzi L, Sun JP, Nihoyannopoulos P, Merlino J, et al. Results of the Predictors of Response to CRT (PROSPECT) trial. Circulation 2008;117:2608-16.
6. Diaz-Infante E, Mont L, Leal J, Garcia-Bolao I, Fernandez-Lozano I, Hernandez-Madrid A, et al. Predictors of lack of response to resynchronization therapy. Am J Cardiol 2005;95:1436-40.
7. Pitzalis MV, Iacoviello M, Romito R, Massari F, Rizzon B, Luzzi G, et al. Cardiac resynchronization therapy tailored by echocardiographic evaluation of ventricular asynchrony. J Am Coll Cardiol 2002;40:1615-22.
8. Yu CM, Fung JW, Zhang Q, Chan CK, Chan YS, Lin H, et al. Tissue Doppler imaging is superior to strain rate imaging and postsystolic shortening on the prediction of reverse remodeling in both ischemic and nonischemic heart failure after cardiac resynchronization therapy. Circulation 2004;110:66-73.
9. Yu CM, Zhang Q, Chan YS, Chan CK, Yip GW, Kum LC, et al. Tissue doppler velocity is superior to displacement and strain mapping in predicting left ventricular reverse remodeling response after cardiac resynchronization therapy. Heart 2006;92:1452-6.
10. Penicka M, Bartunek J, De Bruyne B, Vanderheyden M, Goethals M, De Zutter M, et al. Improvement of left ventricular function after cardiac resynchronization therapy is predicted by tissue doppler imaging echocardiography. Circulation 2004;109:978-83.
11. Tatsumi K, Tanaka H, Yamawaki K, Ryo K, Omar AM, Fukuda Y, et al. Utility of comprehensive assessment of strain dyssynchrony index by speckle tracking imaging for predicting response to cardiac resynchronization therapy. Am J Cardiol 2011;107:439-46.
12. Auger D, Bertini M, Marsan NA, Hoke U, Ewe SH, Thijssen J, et al. Prediction of response to cardiac resynchronization therapy combining two different three-dimensional analyses of left ventricular dyssynchrony. Am J Cardiol 2011;108:711-7.
13. Bleeker GB, Kaandorp TA, Lamb HJ, Boersma E, Steendijk P, de Roos A, et al. Effect of posterolateral scar tissue on clinical and echocardiographic improvement after cardiac resynchronization therapy. Circulation 2006;113:969-76.
14. White JA, Yee R, Yuan X, Krahn A, Skanes A, Parker M, et al. Delayed enhancement magnetic resonance imaging predicts response to cardiac resynchronization therapy in patients with intraventricular dyssynchrony. J Am Coll Cardiol 2006;48:1953-60.
15. Ypenburg C, Roes SD, Bleeker GB, Kaandorp TA, de Roos A, Schalij MJ, et al. Effect of total scar burden on contrast-enhanced magnetic resonance imaging on response to cardiac resynchronization therapy. Am J Cardiol 2007;99:657-60.
16. Birnie DH, de Kemp R, Ruddy TD, Tang AS, Williams K, Guo A, et al. Effect of lateral wall scar on reverse remodeling with cardiac resynchronization therapy. Heart Rhythm 2009;6:1721-6.
17. Prinzen FW, Augustijn CH, Arts T, Allessie MA, Reneman RS. Redistribution of myocardial fiber strain and blood flow by asynchronous activation. Am J Physiol 1990;259:H300-8.
18. Prinzen FW, Hunter WC, Wyman BT, McVeigh ER. Mapping of regional myocardial strain and work during ventricular pacing: Experimental study using magnetic resonance imaging tagging. J Am Coll Cardiol 1999;33:1735-42.
19. Wyman BT, Hunter WC, Prinzen FW, McVeigh ER. Mapping propagation of mechanical activation in the paced heart with MRI tagging. Am J Physiol 1999;276:H881-91.
20. Inoue N, Takahashi N, Ishikawa T, Sumita S, Kobayashi T, Matsushita K, et al. Reverse perfusion-metabolism mismatch predicts good prognosis in patients undergoing cardiac resynchronization therapy: A pilot study. Circ J 2007;71:126-31.
21. Thompson K, Saab G, Birnie D, Chow BJ, Ukkonen H, Ananthasubramaniam K, et al. Is septal glucose metabolism altered in patients with left bundle branch block and ischemic cardiomyopathy? J Nucl Med 2006;47:1763-8.
22. Neri G, Zanco P, Bertaglia E, Zerbo F, Zanon F, Buchberger R. Myocardial perfusion and metabolic changes induced by conventional right and biventricular pacing in dilated cardiomyopathy evaluated by positron emission tomography. Ital Heart J 2002;3:637-42.
23. Nowak B, Sinha AM, Schaefer WM, Koch KC, Kaiser HJ, Hanrath P, et al. Cardiac resynchronization therapy homogenizes myocardial glucose metabolism and perfusion in dilated cardiomyopathy and left bundle branch block. J Am Coll Cardiol 2003;41:1523-8.
24. Neri G, Zanco P, Zanon F, Buchberger R. Effect of biventricular pacing on metabolism and perfusion in patients affected by dilated cardiomyopathy and left bundle branch block: Evaluation by positron emission tomography. Europace 2003;5:111-5.
25. Beanlands RS, Ruddy TD, de Kemp RA, Iwanochko RM, Coates G, Freeman M, et al. Positron emission tomography and recovery following revascularization (PARR-1): The importance of scar and the development of a prediction rule for the degree of recovery of left ventricular function. J Am Coll Cardiol 2002;40:1735-43.
26. Beanlands RS, Nichol G, Huszti E, Humen D, Racine N, Freeman M, et al. F-18-fluorodeoxyglucose positron emission tomography imaging-assisted management of patients with severe left ventricular dysfunction and suspected coronary disease: A randomized, controlled trial (PARR-2). J Am Coll Cardiol 2007;50:2002-12.
27. Massardo T, Gal RA, Grenier RP, Schmidt DH, Port SC. Left ventricular volume calculation using a count-based ratio method applied to multigated radionuclide angiography. J Nucl Med 1990;31:450-6.
28. Lalonde M, Birnie D, Ruddy TD, de Kemp RA, Wassenaar RW. SPECT blood pool phase analysis can accurately and reproducibly quantify mechanical dyssynchrony. J Nucl Cardiol 2010;17:803-10.
29. Bashore TM, Stine RA, Shaffer PB, Bush CA, Leier CV, Schaal SF. The noninvasive localization of ventricular pacing sites by radionuclide phase imaging. Circulation 1984;70:681-94.

30. Botvinick EH, Frais MA, Shosa DW, O'Connell JW, Pacheco-Alvarez JA, Scheinman M, et al. An accurate means of detecting and characterizing abnormal patterns of ventricular activation by phase image analysis. Am J Cardiol 1982;50:289-98.
31. Machac J, Bacharach SL, Bateman TM, Bax JJ, Beanlands R, Bengel F, et al. Positron emission tomography myocardial perfusion and glucose metabolism imaging. J Nucl Cardiol 2006;13:e121-51.
32. Klein R, Lortie M, Adler A, Beanlands R, deKemp R. Fully automated software for polar-map registration and sampling from PET images. IEEE Nucl Sci Symp Conf Rec 2006;6:3185-8.
33. Dilsizian V, Bacharach SL, Beanlands RS, Bergmann SR, Delbeke D, Gropler RJ, et al. PET myocardial perfusion and metabolism clinical imaging. J Nucl Cardiol 2009;16:651.
34. Vitale GD, de Kemp RA, Ruddy TD, Williams K, Beanlands RS. Myocardial glucose utilization and optimization of (18)F-FDG PET imaging in patients with non-insulin-dependent diabetes mellitus, coronary artery disease, and left ventricular dysfunction. J Nucl Med 2001;42:1730-6.
35. Kerlan JE, Sawhney NS, Waggoner AD, Chawla MK, Garhwal S, Osborn JL, et al. Prospective comparison of echocardiographic atrioventricular delay optimization methods for cardiac resynchronization therapy. Heart Rhythm 2006;3:148-54.
36. Cerqueira MD, Weissman NJ, Dilsizian V, Jacobs AK, Kaul S, Laskey WK, et al. Standardized myocardial segmentation and nomenclature for tomographic imaging of the heart: A statement for healthcare professionals from the Cardiac Imaging Committee of the Council on Clinical Cardiology of the American Heart Association. Circulation 2002;105:539-42.
37. Altehoefer C, vom DJ, Buell U. Septal glucose metabolism in patients with coronary artery disease and left bundle-branch block. Coron Artery Dis 1993;4:569-72.
38. Zanco P, Desideri A, Mobilia G, Cargnel S, Milan E, Celegon L, et al. Effects of left bundle branch block on myocardial FDG PET in patients without significant coronary artery stenoses. J Nucl Med 2000;41:973-7.
39. Depre C, Shipley GL, Chen W, Han Q, Doenst T, Moore ML, et al. Unloaded heart in vivo replicates fetal gene expression of cardiac hypertrophy. Nat Med 1998;4:1269-75.
40. Bleeker GB, Mollema SA, Holman ER, Van d Veire N, Ypenburg C, Boersma E, et al. Left ventricular resynchronization is mandatory for response to cardiac resynchronization therapy: Analysis in patients with echocardiographic evidence of left ventricular dyssynchrony at baseline. Circulation 2007;116:1440-8.
41. Chen J, Bax JJ, Henneman MM, Boogers MJ, Garcia EV. Is nuclear imaging a viable alternative technique to assess dyssynchrony? Europace 2008;10:iii101-5.
42. Henneman MM, Chen J, Ypenburg C, Dibbets P, Bleeker GB, Boersma E, et al. Phase analysis of gated myocardial perfusion single-photon emission computed tomography compared with tissue Doppler imaging for the assessment of left ventricular dyssynchrony. J Am Coll Cardiol 2007;49:1708-14.
43. Sutton MG, Plappert T, Hilpisch KE, Abraham WT, Hayes DL, Chinchoy E. Sustained reverse left ventricular structural remodeling with cardiac resynchronization at one year is a function of etiology: Quantitative Doppler echocardiographic evidence from the Multicenter InSync Randomized Clinical Evaluation (MIRACLE). Circulation 2006;113:266-72.